

ORIGINAL ARTICLE

The Yucatan Minipig Temporomandibular Joint Disc Structure–Function Relationships Support Its Suitability for Human Comparative Studies

Natalia Vapniarsky, DVM, DACVP,¹ Ashkan Aryaei, PhD,¹ Boaz Arzi, DVM, DAVDC, DEVDC²
David C. Hatcher, DDS, MSc, MRCD(c),^{2,3} Jerry C. Hu, PhD,¹ and Kyriacos A. Athanasiou, PhD^{1,4}

Frequent involvement of the disc in temporomandibular joint (TMJ) disorders warrants attempts to tissue engineer TMJ disc replacements. Physiologically, a great degree of similarity is seen between humans and farm pigs (FPs), but the pig's rapid growth confers a significant challenge for *in vivo* experiments. Minipigs have a slower growth rate and are smaller than FPs, but minipig TMJ discs have yet to be fully characterized. The objective of this study was to determine the suitability of the minipig for TMJ studies by extensive structural and functional characterization. The properties of minipig TMJ discs closely reproduced previously reported morphological, biochemical, and biomechanical values of human and FP discs. The width/length dimension ratio of the minipig TMJ disc was 1.95 (1.69 for human and 1.94 for FP). The biochemical evaluation revealed, on average per wet weight, 24.3% collagen (22.8% for human and 24.9% for FP); 0.8% glycosaminoglycan (GAG; 0.5% for human and 0.4% for FP); and 0.03% DNA (0.008% for human and 0.02% for FP). Biomechanical testing revealed, on average, compressive relaxation modulus of 50 kPa (37 kPa for human and 32 kPa for FP), compressive instantaneous modulus of 1121 kPa (1315 kPa for human and 1134 kPa for FP), and coefficient of viscosity of 13 MPa·s (9 MPa·s for human and 3 MPa·s for FP) at 20% strain. These properties also varied topographically in accordance to those of human and FP TMJ discs. Anisotropy, quantified by bidirectional tensile testing and histology, again was analogous among minipig, human, and FP TMJ discs. The minipig TMJ's ginglymoarthrodial nature was verified through cone beam computer tomography. Collectively, the similarities between minipig and human TMJ discs support the use of minipig as a relevant model for TMJ research; considering the practical advantages conferred by its growth rate and size, the minipig may be a preferred model over FP.

Keywords: temporomandibular joint disc, characterization, structure–function, large animal model, translation, anisotropy

Introduction

TEMPOROMANDIBULAR JOINT (TMJ) disorders, or TMD, are a heterogeneous group of pathologies involving the TMJ and, potentially, its associated muscles.¹ According to the NIH epidemiology report, the prevalence of TMD affects 5% to 12% of the population worldwide.² TMD's comorbidities, for example, headache/migraine, neck, and TMJ pain³ result in marginal to significant disability and substantial healthcare costs.⁴ TMJ disc displacement

and inflammatory degenerative disorders have been diagnosed in 41% and 31% of TMD patients worldwide, respectively.¹

TMD management options vary with respect to disease severity, ranging from symptomatic therapy to invasive surgery.⁵ Total joint replacement with prosthetics or TMJ disc removal are currently the only options available at late-stage TMD.⁶ None of these treatments offer complete resolution and repeat or follow-up surgeries may be required.⁷ Novel regenerative solutions, preferably applicable to earlier stages

¹Department of Biomedical Engineering, University of California, Davis, Davis, California.

²Department of Surgical and Radiological Sciences, School of Veterinary Medicine, University of California, Davis, Davis, California.

³Diagnostic Digital Imaging Center, Sacramento, California.

⁴Department of Orthopedic Surgery, School of Medicine, University of California, Davis, Davis, California.

of TMD, are needed. Unfortunately, introduction of new regenerative solutions for TMD requires the use of an appropriate animal model, which can be costly. For these animals, joint anatomy and loading patterns need to be comparable to humans, and long-term follow-up would be required.

The farm pig (FP) model is often used in biomedical research and has enjoyed popularity in dentistry and maxillofacial surgery research.⁸ FP's omnivorous nutrition, anatomical similarities, physiology, and bone biology all resemble those of humans, making them exceedingly suited for maxillofacial research.⁹ Like higher primates, pigs have bilateral occlusion at full closure, a symphysis that fuses after infancy, and sliding joint mechanics.¹⁰ Furthermore, the chewing pattern of pigs closely resembles that of humans and primates.¹¹ This is in contrast to ruminants (e.g., cow, goat, and sheep). Miniature varieties (i.e., minipigs) of *Sus scrofa domestica* (i.e., FPs) may be more suitable for long-term studies since the significant and rapid growth of FPs renders it impractical in terms of handling, housing space requirements, surgery, anesthesia, and food costs.⁸

Because of the complex loading patterns that engineered tissues are expected to experience in the TMJ, acquisition of complete design parameters from native tissue is critical. In recognition of this, several studies characterizing the properties of TMJ discs in farm animals and humans have been performed,^{12,13} and efforts to engineer biologically functional tissue have generated promising results.^{14–18} These do not include the minipig. The TMJ disc of minipigs has never been fully characterized, despite this model's practical advantages (e.g., size, growth rate, and ease of handling).

To this end, this work characterized the TMJ disc of Yucatan minipigs by performing extensive structure-function analysis of the native tissue. Minipig TMJ discs were investigated by gross morphology, microscopic and ultrastructural morphology, biochemical analysis, and mechanical testing under tension and compression. Furthermore, examinations of anisotropy (biomechanically and microscopically) and the degree of collagen crosslinking in different anatomic regions were also performed. We hypothesized that the properties of the minipig TMJ discs would closely mimic those of human TMJ discs. By extension, we hypothesized that structural characteristics, for example, GAG and collagen content, and collagen crosslinking, would correlate with the mechanical properties to provide greater insight on the tissue's function *in situ*. This work should provide a substantial contribution toward our understanding of the structure–function of the TMJ, assisting the generation of novel regenerative solutions for human TMD.

Materials and Methods

Animals, TMJ disc gross morphology, and cone beam computer tomography

TMJ discs were obtained from eight healthy, skeletally mature, 16- to 18-month-old male Yucatan minipigs that were sacrificed due to reasons unrelated to this study. The skeletal maturity was verified grossly by examination of the distal femoral and proximal tibial epiphyses for closure.¹⁹ The discs were excised *en bloc*, as previously described.²⁰ Samples were taken from anterior (A), posterior (P), lateral (L), medial (M), and central (C) regions for analyses. Before TMJ excision, structural elements of the TMJ were evalu-

ated using cone beam computer tomography (CBCT). Intact cadaver heads were imaged in open- and closed-mouth positions with or without contrast arthrography, performed by injection of 1.5 mL of Isovue (Iopamidol, Bracco Diagnostics, Inc., NJ) into the inferior and superior joint spaces (see Supplementary Data for more details; Supplementary Data are available online at www.liebertpub.com/tec). Deidentified images of human CBCT scans and X-rays were courtesy of Dr. David C. Hatcher.

Histology, immunohistochemistry, and ultrastructure

Samples fixed in 10% buffered formalin were paraffin embedded and sectioned at 5 μ m in the superoinferior (dorsoventral), mediolateral, and horizontal planes, and stained using hematoxylin and eosin (H&E), Safranin-O/Fast green, PicroSirius Red, and Verhoeff Van Gieson.²¹ For immunohistochemistry (IHC), sections were labeled with anti-bovine collagen type I (ab90395, 1:3000; Abcam, Cambridge, MA), anti-human collagen type II (ab34712, 1:500; Abcam) antibodies, and anti-human Factor 8 (F8/86, 1:2000; Dako, Santa Clara, CA).

For scanning electron microscopy (SEM), sections from each anatomic region were fixed in 3% glutaraldehyde (Sigma, St. Louis, MO), dehydrated, and cryofractured²⁰ in orientations specified in Figure 5a. The cryofracture procedure allowed for examination of the collagen fiber alignment at the surface and depth of the disc. Cryofractured sections were mounted, critical point-dried, and sputter-coated with gold before viewing on a Philips XL30 TMP SEM. Fiber thicknesses in each anatomic location were measured from images at 12,000 \times magnification with Image J software (NIH Bethesda, MD).

Compressive mechanical testing

Uniaxial, unconfined stress relaxation compressive testing was performed on an Instron 5565 (Instron, Norwood, MA) using 3 mm diameter cylindrical samples representing the five anatomic regions of the disc.¹³ Throughout testing, samples were submerged in isotonic saline at room temperature. Following the application of 10% and 20% strain at 10%/s of sample thickness, platen position was maintained for 600 and 1200s, respectively, for relaxation to reach equilibrium. A custom MATLAB (MathWorks, Natick, MA) code developed to fit the data to the Kelvin solid viscoelastic model was used to establish instantaneous modulus (E_i), relaxation modulus (E_r), and coefficient of viscosity (η) at each strain level.¹³

Tensile mechanical testing

Uniaxial tensile testing was performed on dog bone-shaped samples in two perpendicular directions (anteroposterior and mediolateral) from the five anatomic regions of the disc. Samples were elongated at a rate of 1%/s of gauge length until failure. The stress–strain curves generated from the load–displacement data were analyzed with a custom program on MATLAB²⁰ to determine Young's modulus (E_Y) and ultimate tensile strength (UTS).

Anisotropy measurement

An anisotropy index (AI) was calculated by dividing the absolute value of the difference between the tensile properties

in the two tested directions, divided by the larger of the two tensile values:

$$AI = \frac{Abs (direction 1 - direction 2)}{Max (direction 1, direction 2)}$$

Values approaching 1.0 were indicative of strong anisotropy, while values approaching 0.0 indicated isotropy.

Biochemistry

Biochemical assays were performed as previously described.¹³ Samples were digested in 125 µg/mL papain (Sigma) in phosphate buffer. GAG content was measured with Blyscan GAG assay (Bicolor, Westbury, NY) based on 1, 9-dimethylmethyl blue binding. The total collagen was quantified after sample hydrolysis with 2N NaOH for 20 min at 110°C, using a chloramine-T hydroxyproline assay with Sircol™ collagen standards (Bicolor). PicoGreen assay (Invitrogen, Carlsbad, CA) was used to assess total DNA content.

Collagen crosslinking measurement

Collagen crosslinking was evaluated by quantification of pyridinoline using high-performance liquid chromatography,²² using pyridinoline standards (Quidel, San Diego, CA).

Statistical analysis

To determine regional differences in collagen, GAG content, compressive and tensile properties, and pyridinoline concentration, one-way analysis of variance (ANOVA) across all anatomic locations was performed for each property. Tukey's *post hoc* analysis was performed when indicated ($\alpha=0.05$). To determine the presence of anisotropy, tensile properties in the anteroposterior direction were compared to those in mediolateral direction using Student's *t*-test ($\alpha=0.05$), for each anatomic region. All data are presented as mean \pm standard deviation.

Results

Gross morphology and CBCT

The minipig TMJ discs were oval and biconcave, with dimensions of 25.6 and 13.1 mm in the anteroposterior and mediolateral directions (Fig. 1 and Supplementary Table S1). Thicknesses varied from 1.6 to 5.9 mm in the center and at the periphery of the disc, respectively (Fig. 1 and Supplementary Table S1).

CBCT evaluation demonstrated translation/gliding movement of the mandibular head anteriorly and under the articular eminence in human and minipig species during mouth opening (Fig. 2). In addition, repeated scans following injection of the contrast material into the superior and inferior joint spaces further highlighted anatomical similarities between human and minipig species (Supplementary Fig. S2).

Histology, IHC, and SEM

The disc central areas were paucicellular and primarily avascular. The collagen fibers were arranged in an orthogonally intercepting pattern in all, but the central region. In the central region, the fiber orientation was almost exclu-

sively anteroposterior with occasional islands of basophilic matrix with chondrocyte-like cells (Supplementary Fig. S1). Fiber orientation observed using H&E was confirmed with PicroSirius Red staining under polarized light (Fig. 1). Staining for GAGs revealed faint, multifocal Safranin O positivity. The Verhoeff Van Gieson stain highlighted the presence of elastic fibers across all regions, with a higher concentration of fibers in the posterior region (Supplementary Fig. S1). The elastic fibers in the anterior, central, medial, and lateral areas were primarily near the articular surfaces of the disc and around larger vessels. IHC revealed strong immunoreactivity for collagen type I and faint immunoreactivity for collagen type II (Fig. 1). Immunolabeling for Factor VIII highlighted the presence of larger blood vessels in the anterior and posterior regions, and smaller vessels in the lateral, medial, and central regions of the disc (Supplementary Fig. S1). SEM evaluation confirmed the aforementioned fiber orientation and crimping. The average thickness of collagen fibers was significantly higher in the anterior and posterior bands (Fig. 5).

Biochemistry

The disc contained collagen throughout, with the highest concentration of 26.69%/WW and 27.80%/WW found in the central and posterior regions, respectively (Fig. 3 and Supplementary Table S2). The medial region had significantly lower collagen content. No significant difference in GAG/WW was detected among regions, although medial, lateral, and central regions trended slightly higher (Fig. 3 and Supplementary Table S2). DNA content varied between 0.024%/WW in the posterior and 0.041%/WW in the medial regions with no significant difference among regions (Fig. 3 and Supplementary Table S2).

Crosslinking

Pyridinoline content, normalized to collagen content, was significantly lower in the anterior and posterior regions than in the lateral and medial regions (Fig. 3). Because pyridinoline content was not normally distributed on the residual plot, Box-Cox transformation was performed to achieve normality. Once the assumption of normal distribution was met, ANOVA with Tukey's *post hoc* analysis was applied on the means of the transformed variables.

Mechanical testing

Compressive mechanical testing revealed significantly higher relaxation and instantaneous moduli in the anterior and posterior regions at 20% strain. Instantaneous and relaxation moduli for 20% strain ranged from 216 kPa in the central region to 1540 kPa in the posterior region, and from 20.5 kPa in the medial region to 57.5 kPa in the anterior region, respectively (Fig. 4 and Supplementary Table S3).

Tensile properties among regions were compared with respect to direction of testing using ANOVA. Analysis revealed that the central region was significantly stiffer and stronger than any other regions in the anteroposterior direction, while the posterior region was the stiffest and strongest when tested in the mediolateral direction (Supplementary Fig. S2).

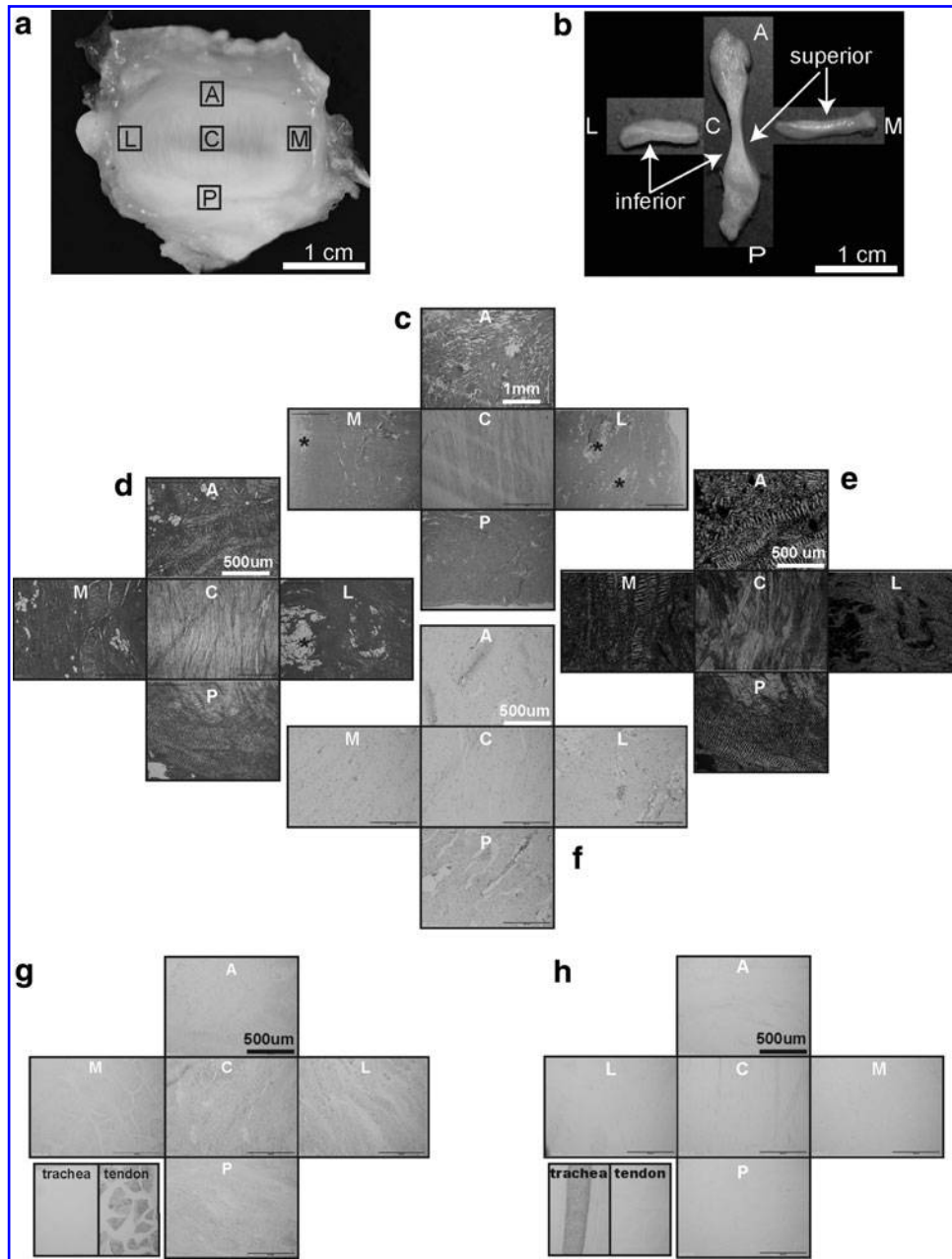


FIG. 1. Gross morphology, cross sectional parameters, histology, histochemistry, and immunohistochemistry of the minipig TMJ disc. *Capital letters* represent anatomic regions of the disc: A, anterior; C, central; L, lateral; M, medial; P, posterior. **(a)** Superior surface view of the whole intact normal minipig TMJ disc. **(b)** Minipig TMJ disc sectioned in the anteroposterior and mediolateral directions demonstrating a biconcave morphology. **(c)** Representative horizontal hematoxylin and eosin sections from five anatomic regions of the minipig TMJ disc (scale bar=1 mm). This panel demonstrates (1) distinct and an almost exclusively anteroposterior orientation of the collagen fibers in the central region and (2) fiber orientation primarily perpendicular to the sectioning plane in the lateral, medial, and posterior regions. Occasional small adipose tissue islands (*) are present in the lateral and medial regions of the disc. **(d, e)** PicroSirius Red staining of the horizontal disc sections highlights the previously described collagen fiber orientation and crimping of the collagen fibers viewed under regular and polarized light, respectively. **(f)** Safranin O/Fast Green staining of the horizontal disc sections demonstrates very faint positive staining for GAGs in all disc regions. **(g)** Collagen type I immunolabeling performed on the horizontal sections of the disc demonstrates diffused immunopositivity across all disc regions. Negative tissue control (trachea) demonstrates no immunopositivity, while positive tissue control (tendon) is immunoreactive for this antigen. **(h)** Collagen type II immunolabeling performed on the horizontal sections of the disc demonstrates minimal immunoreactivity for collagen type II in all disc regions. The positive tissue control (trachea) is strongly immunoreactive, while negative tissue control (tendon) shows no immunoreactivity. GAGs, glycosaminoglycans; TMJ, temporomandibular joint.

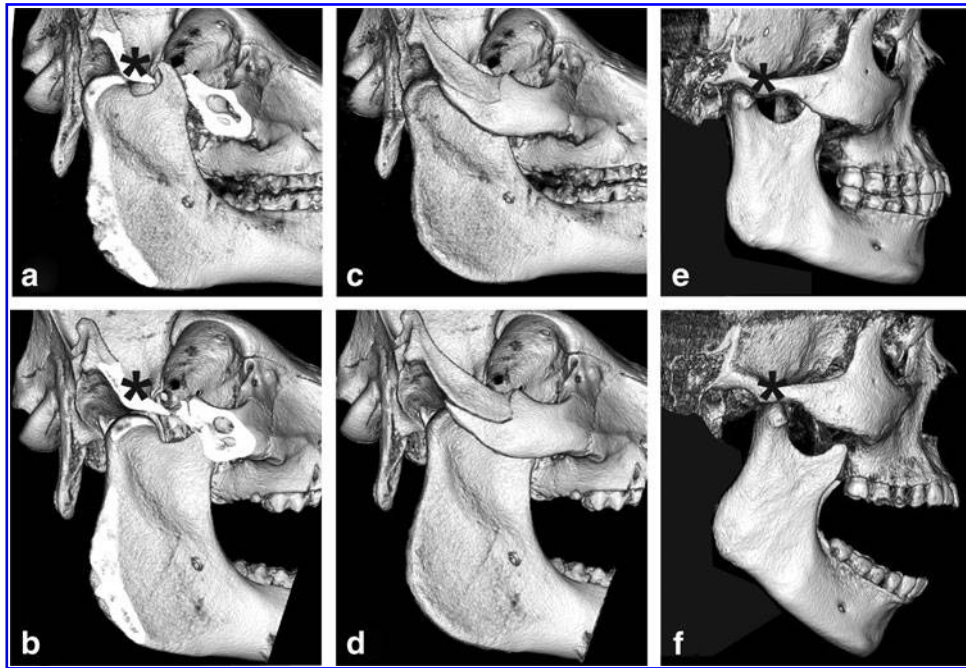


FIG. 2. Cone beam computer tomography (CBCT) three-dimensional reconstruction of human and minipig skulls in open and closed-mouth positions. (a, c) Minipig skull in closed-mouth position. Part of the zygomatic arch was digitally removed in (a) to demonstrate joint inaccessibility using lateral surgical approaches. It is noted that the width of the condylar neck is larger than in the human (e). (b, d) Minipig skull in open-mouth position. With the zygomatic arch digitally removed (d), the translational/gliding movement of the mandibular head anteriorly toward and under the articular eminence (*) is evident. To better appreciate the translational movement, it is instructive to compare the positions of the mandibular head on images (a, b). (e) Human skull in a closed-mouth position. The lack of a prominent zygomatic arch is suggestive of a relatively easy lateral surgical approach. Also notable is the smaller width of the human condylar neck. (f) Human skull in open-mouth position demonstrating translational gliding movement of the mandibular head anteriorly toward and under the articular eminence (*). The human CBCT images are courtesy of David C. Hatcher.

Anisotropy

For the assessment of anisotropy, tensile properties of each region were collected from two testing directions. For each region, directional data were then compared using Student's *t*-test (Fig. 4 and Supplementary Table S4). In the anteroposterior direction, the tensile properties of the central region of the disc were significantly higher (UTS of 20.5 MPa and Young's modulus of 31.0 MPa) than in the mediolateral direction (UTS of 1.2 MPa and Young's modulus of 1.8 MPa). The posterior region was significantly stiffer and stronger in the mediolateral direction than in the anteroposterior direction. Surprisingly, no significant difference in tensile stiffness was detected between two testing directions in the anterior region. This bidirectional tensile testing yielded AI values ranging from 0.4 in the anterior band to 0.9 and 0.8 in the central and posterior regions, respectively (Fig. 5 and Supplementary Table S5).

Discussion

The objective of this study was to determine the suitability of the minipig as an animal model for research related to the human TMJ disc. This was performed through extensive characterization of the TMJ disc of Yucatan minipigs. Methods corresponding to those previously used to characterize the human and FP^{12,13} TMJ disc were selected to allow side-by-side comparison of morphological, biochemical, and mechanical parameters. In addition, pre-

viously unexplored characteristics such as degree of collagen crosslinking, AI, and cone beam computer tomography scanning were applied to yield novel information regarding the minipig TMJ disc and joint. Our hypothesis that the properties of minipig TMJ disc will correspond closely to those of humans and FPs was supported by the data; the TMJ disc of Yucatan minipigs was found to have morphological, histological, biochemical, and mechanical properties that are close to those of human and FPs.

Morphological and histological features of the minipig were remarkably similar to human and FP TMJ discs. Importantly, the average adult human body mass in United States is 82 kg,²³ while adult FP body mass is 150–300 kg at skeletal maturity.²⁴ The Yucatan minipig's body mass is 82 kg.²⁴ Despite humans and minipigs having large differences in body mass when compared to FPs, their TMJ discs did not scale proportionately. The width-to-length ratios of the human, FP, and minipig TMJ disc were 1.69, 1.94, and 1.95, respectively. Proportionally, disc size to body mass was more similar between minipigs and humans than between FPs and humans. Other morphological features, such as the intensity of GAG staining among the disc regions, scarcity of collagen type II, and abundance of collagen type I of the minipig TMJ disc also closely traced the properties of human and FP discs.^{13,25} Collagen orientation in the minipig disc was anteroposterior in the central, lateral, and medial regions, and mediolateral in the posterior band (Fig. 1), as previously reported for humans and FPs.^{13,26} The distribution

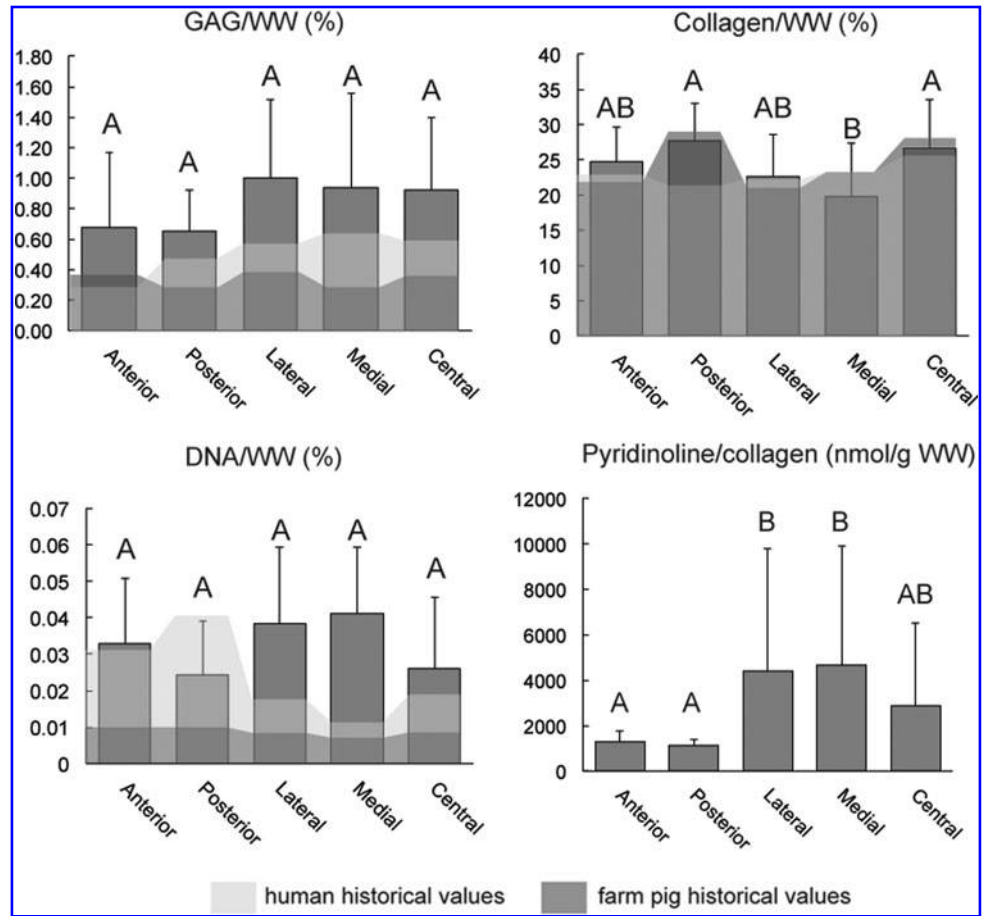


FIG. 3. Biochemistry. GAG/WW, collagen/WW, DNA/WW, and pyridinoline/collagen across five anatomic locations of the minipig TMJ disc are shown with respect to historical values reported for human (*light shade*) and farm pig (*dark shade*) TMJ discs. Columns labeled with different letters are significantly different.

of elastic fibers in minipig discs resembled that of humans, which was higher in the anterior and posterior regions²⁷ (Supplementary Fig. S1).

CBCT imaging of different mouth positions confirmed that the minipig TMJ experiences both rotation and translation (Fig. 2). This motion was not reported in other commonly used experimental animal models, except for primates²⁸ and rabbits.²⁹ For the cow and smaller herbivores, jaw movement is primarily mediolateral; in dogs, it is mainly of a hinge-like type.²⁸ The CBCT data agree with prior work performed using a more invasive methodology.³⁰ These morphological similarities support the minipig's use as a model for TMJ disc biomedical research.

Despite their similarities, minipig and human TMJ display important anatomical differences. These include the size and positioning of the zygomatic arch and the width of the neck of the condylar process (Fig. 2). In humans, the zygomatic arch was $\sim 14.04 \text{ mm}^2$ in cross-section, while in the FPs and minipigs, the zygomatic arch was $\sim 97.03 \text{ mm}^2$ and partially obscured the lateral aspect of the joint. The width of the neck of the condylar process was twice narrower in humans than in minipigs, with cross-sectional areas of 76.41 mm^2 and 150.32 mm^2 at the narrowest point, respectively. These details are important for developing a surgical approach to the minipig TMJ. The lateral preauricular approach is most commonly employed for human TMJ surgery.³¹ This approach does not translate to minipigs because the zygomatic arch precludes lateral access to the TMJ³⁰ (Fig. 2). If the minipig is used in condylectomy models, the width of the

condylar process also should be considered. These differences should not discourage use of the minipig model, but must be kept in mind during experimental design.

Biochemical and biomechanical properties of minipig TMJ discs bore striking similarities to historical values of human and FP TMJ discs. The GAG content of minipig discs was low ($1\%/DW$) in comparison to articular cartilage ($30\%/DW$)³² or knee meniscus ($17\%/DW$)³³; similarly, low GAG content was found in human and FP discs.¹³ The collagen/GAG ratio for the minipig disc was 28.9, which is more similar to humans (43.0) than FPs (67.3) (Fig. 3 and Supplementary Table S2).¹³ For human articular cartilage, this ratio was 3.3,¹² highlighting the differences in function between TMJ discs and articular cartilage. Although no statistical difference in GAG content was detected among anatomical regions of the minipig disc, GAG content in the central, medial, and lateral regions trended higher, consistent with histological observations and with previous reports in humans.³⁴ For humans, FPs, and minipigs, compressive moduli of the disc anterior and posterior regions were significantly higher (four to nine times) than central, medial, and lateral regions (Fig. 4 and Supplementary Table S3). In agreement with historical reports on human and FP discs, central portions of minipig discs were 50-fold stiffer in tension than in compression (Fig. 4 and Supplementary Table S4). Human TMJ discs trended lower in DNA content than pig discs, which is likely due to age-related cellularity decreases³⁵; the average age for human specimens was 73 years,¹³ while the average age for minipigs was 1.5 years.

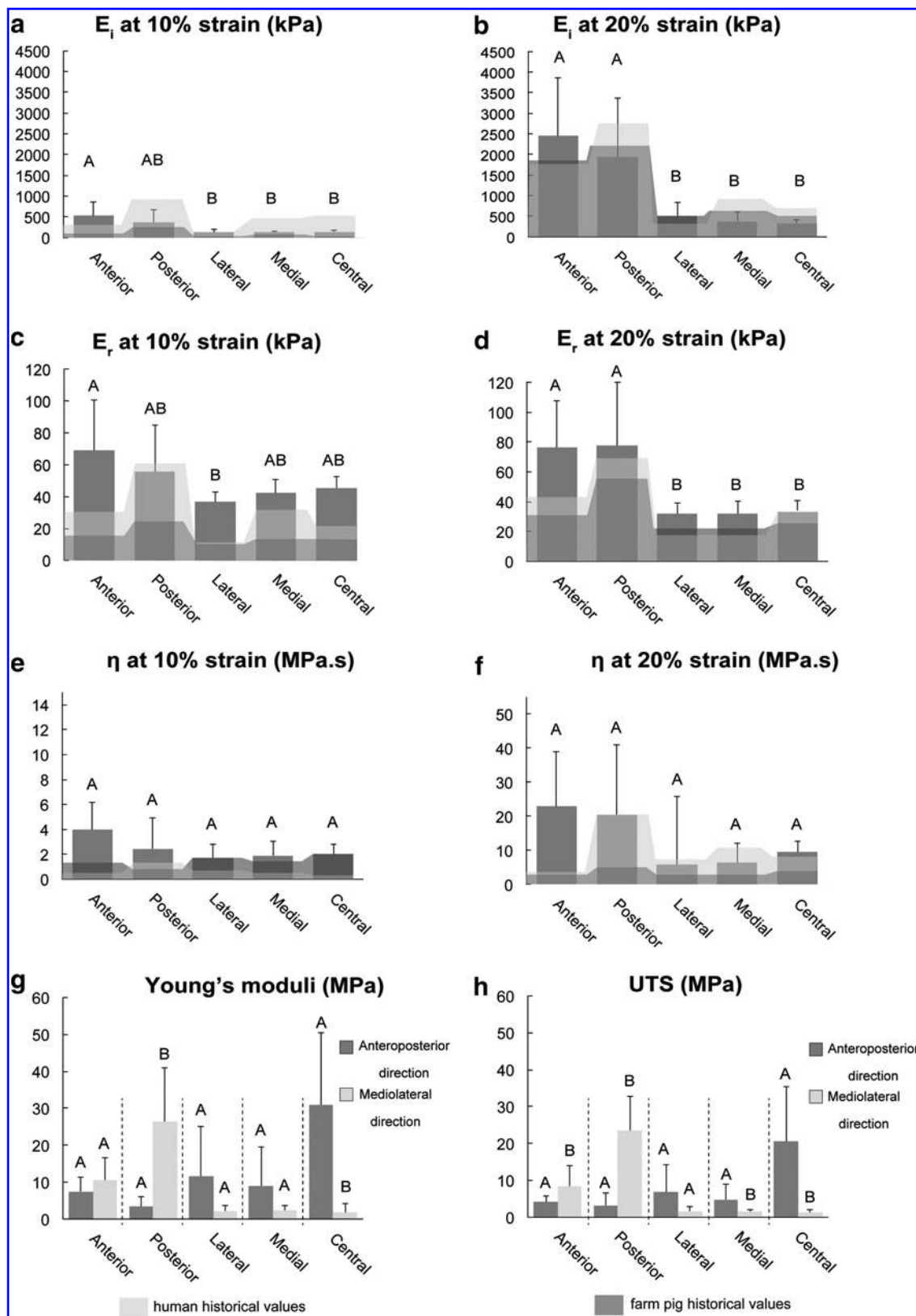


FIG. 4. Biomechanics. Instantaneous modulus (E_i), relaxation modulus (E_r), and coefficient of viscosity (η) values at 10% and 20% strain are shown in (a–f). Historical values for humans and farm pigs are shown as background reference values in *light shade* and *dark shade*, respectively; (g, h) tensile stiffness (Young’s modulus) and ultimate tensile strength (UTS) of the five anatomic regions of the minipig TMJ tested in two perpendicular directions (direction AP, anteroposterior; direction ML, mediolateral). Each region was analyzed separately using Student’s *t*-test to determine difference between two perpendicular testing directions. It is notable that tensile stiffness and tensile strength of the central area of the disc are 30-fold higher in the AP direction than in the ML direction. Columns labeled with different capital letters are significantly different.

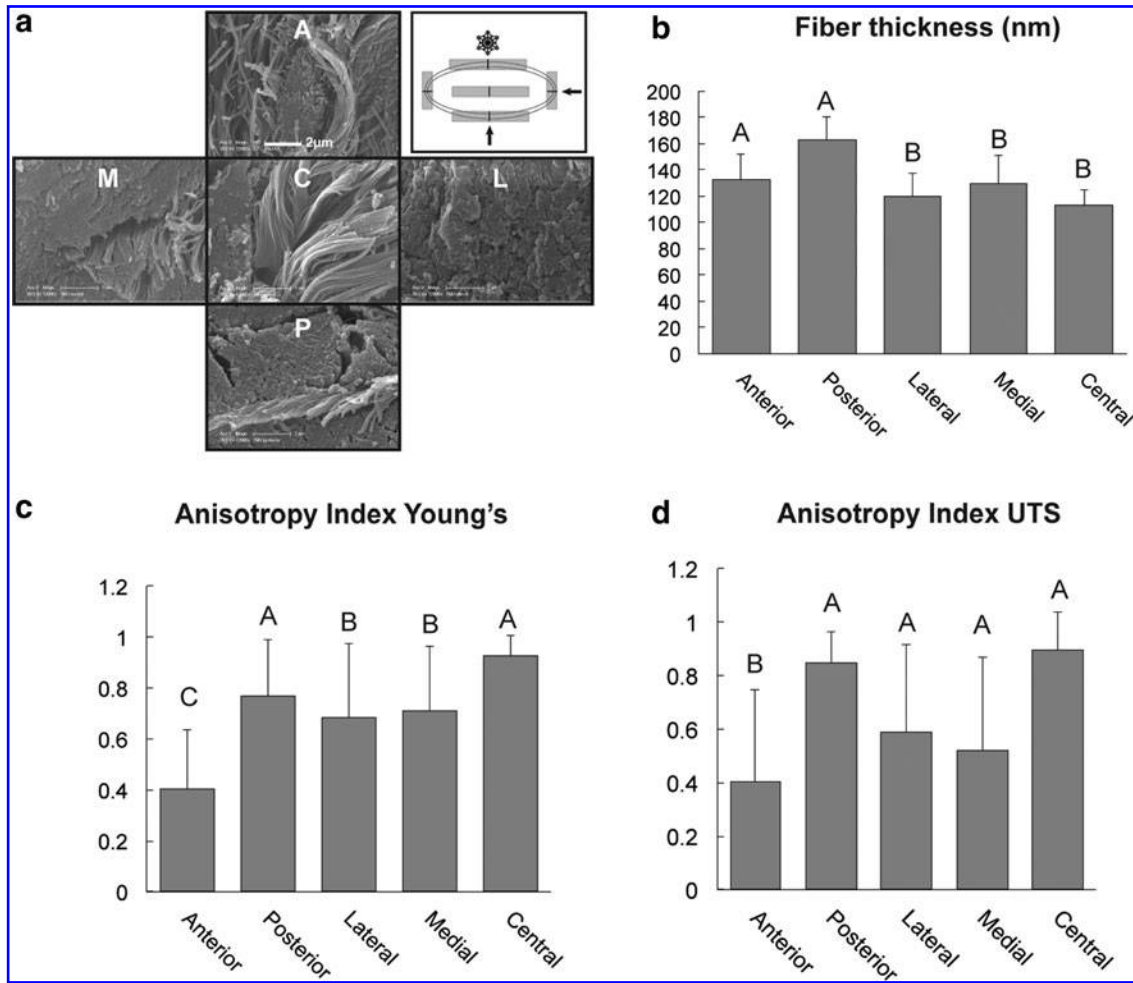


FIG. 5. Anisotropy of fiber orientation demonstrated by scanning electron microscopy and measurement of the anisotropy index (AI) with bidirectional tensile testing. **(a)** Demonstrates the orientation of the collagen fibers in the different anatomic locations of the disc. Also shown is how the disc is processed with cryofracture, and *arrows* indicate the direction of the fracturing plane. Note that in the posterior (P), lateral (L), and medial regions (M), the fibers are oriented perpendicular to the plane of section, while in the central region (C), the fibers are oriented parallel to the plane of section. Mixed organizational patterns are present in the anterior region (A). **(b)** Fiber thickness across different regions of the disc. Note the significantly thicker fiber diameters in the anterior and posterior regions. **(c, d)** Demonstrate the AI calculated from the bidirectional tensile testing values. Note the values approaching “one” represent high degree of anisotropy. Areas with values approaching “zero,” such as the anterior region, possess low degree of anisotropy and thus are more isotropic or directionally independent. In all the charts columns labeled with different capital letters are significantly different.

Collectively, a great degree of similarity was found in terms of biochemical and mechanical properties between minipig and human TMJ discs. This further supports the minipig model for translational biomedical research.

Contrary to the oft-reported structure–function relationship of articular cartilage that correlates GAG content with compressive properties,³⁶ for humans, minipigs, and FPs, the TMJ disc’s compressive properties trended lower in the central regions despite higher GAG content in these regions.^{12,13} Thus, components beside GAGs likely contribute to disc compressive properties; for example, the mean diameter of collagen fibril correlated with the compressive properties of the human intervertebral disc’s annulus fibrosus.³⁷ Our findings, similarly, show that regions with higher compressive properties also had significantly higher fibril diameter (Fig. 5, anterior and posterior regions). Interestingly, these same regions had significantly lower pyr-

idinoline content (Fig. 3). The latter finding agrees with the report that crosslinks tend to be less numerous if the collagen fibrils are thick.³⁸ Such extracellular matrix properties should be examined in greater depth before the TMJ disc’s structure–function relationships can be fully elucidated. Notably, in this study as well as the historical work to which our values were compared, high standard deviations in both compressive and tensile values were observed. It was reported that reduction of strain rate may potentially reduce these standard deviations.³⁹ Therefore, in future experiments, it may be prudent to consider lower rates of loading.

The TMJ disc’s anisotropy is known,^{13,25,40} but rarely quantified. Both FPs and minipigs have similar fiber arrangement to humans based on SEM.²⁶ In this study, tensile testing precisely quantified anisotropy. Bidirectional tensile testing showed that the central and posterior regions were most anisotropic (AI=0.89 and 0.86, respectively), while

the anterior region exhibited isotropy (AI=0.40) (Fig. 5). This is in agreement with another report that quantified anisotropy of FP TMJ discs using fluorescence recovery after photo bleaching.⁴¹ The latter determined posterior and central regions as most anisotropic, in contrast to the anterior region, which was isotropic.⁴¹ It is worth noting that significant regional differences were found in Young's modulus and UTS. Specifically, in the anteroposterior direction of testing, the central region was the stiffest, while in the mediolateral direction, anterior and posterior regions were the stiffest (Supplementary Fig. S2). The quantitative AI enabled by bidirectional tensile testing is useful not only for characterizing animal models in this experiment but can also be extended to study disease progression of the disc.

This study indicates that the minipig is an acceptable animal model for studies related to the human TMJ disc. This finding is bolstered by other reports indicating the suitability of this animal for translational studies. For instance, due to hematological and cardiovascular similarities to humans, minipigs have already been established by the International Organization for Standardization as suitable animal models for investigating medical devices⁴² and are widely accepted as appropriate models for cardiovascular research.⁴³ Increasing numbers of studies use the minipig as a model for reproductive toxicology testing. Minipigs have been deemed as an acceptable nonrodent model for studies of compounds intended for dermal, oral, and parenteral administration by the International Consortium for Innovation and Quality in Pharmaceutical Development.⁴³ In terms of TMJ research, the structural and functional similarities between human and minipig TMJ discs and joints, supplemented by clinically relevant advantages of minipigs in terms of maintenance, size, and suitability for surgical anesthesia and diagnostic procedures, render the minipig not only suitable but more advantageous over FP.

Acknowledgments

We acknowledge Dr. W. Douglas Boyd and Dr. Leigh Griffiths for donating the cadaveric minipig specimens. We also acknowledge the funding from NIH R01DE015038. The authors declare no conflicts of interest related to this report.

Disclosure Statement

No competing financial interests exist.

References

- Manfredini, D., Guarda-Nardini, L., Winocur, E., Piccotti, F., Ahlberg, J., and Lobbezoo, F. Research diagnostic criteria for temporomandibular disorders: a systematic review of axis I epidemiologic findings. *Oral Surg Oral Med Oral Pathol Oral Radiol Endod* **112**, 453, 2011.
- National Institute of Dental and Craniofacial Research. Prevalence of TMJD and Its Signs and Symptoms, 2014. <https://www.nidcr.nih.gov/DataStatistics/FindDataByTopic/FacialPain/PrevalenceTMJD.htm> (accessed June 28, 2017).
- Plesh, O., Adams, S.H., and Gansky, S.A. Temporomandibular joint and muscle disorder-type pain and comorbid pains in a national US sample. *J Orofac Pain* **25**, 190, 2011.
- White, B.A., Williams, L.A., and Leben, J.R. Health care utilization and cost among health maintenance organization members with temporomandibular disorders. *J Orofac Pain* **15**, 158, 2001.
- Aryaei, A., Vapniarsky, N., Hu, J.C., and Athanasiou, K.A. Recent tissue engineering advances for the treatment of temporomandibular joint disorders. *Curr Osteoporos Rep* **14**, 269, 2016.
- Mercuri, L.G. Alloplastic temporomandibular joint replacement: rationale for the use of custom devices. *Int J Oral Maxillofac Surg* **41**, 1033, 2012.
- Henry, C.H., and Wolford, L.M. Treatment outcomes for temporomandibular joint reconstruction after Proplast-Teflon implant failure. *J Oral Maxillofac Surg* **51**, 352, 1993.
- Mardas, N., Dereka, X., Donos, N., and Dard, M. Experimental model for bone regeneration in oral and cranio-maxillo-facial surgery. *J Invest Surg* **27**, 32, 2014.
- Almond, G.W. Research applications using pigs. *Vet Clin North Am Food Anim Pract* **12**, 707, 1996.
- Herring, S.W., Decker, J.D., Liu, Z.J., and Ma, T. Temporomandibular joint in miniature pigs: anatomy, cell replication, and relation to loading. *Anat Rec* **266**, 152, 2002.
- Herring, S.W. The dynamics of mastication in pigs. *Arch Oral Biol* **21**, 473, 1976.
- Willard, V.P., Kalpakci, K.N., Reimer, A.J., and Athanasiou, K.A. The regional contribution of glycosaminoglycans to temporomandibular joint disc compressive properties. *J Biomech Eng* **134**, 011011, 2012.
- Kalpakci, K.N., Willard, V.P., Wong, M.E., and Athanasiou, K.A. An interspecies comparison of the temporomandibular joint disc. *J Dent Res* **90**, 193, 2011.
- MacBarb, R.F., Chen, A.L., Hu, J.C., and Athanasiou, K.A. Engineering functional anisotropy in fibrocartilage neotissues. *Biomaterials* **34**, 9980, 2013.
- Murphy, M.K., Arzi, B., Prouty, S.M., Hu, J.C., and Athanasiou, K.A. Neocartilage integration in temporomandibular joint discs: physical and enzymatic methods. *J R Soc Interface* **12**, pii: 20141075, 2015.
- Kalpakci, K.N., Kim, E.J., and Athanasiou, K.A. Assessment of growth factor treatment on fibrochondrocyte and chondrocyte co-cultures for TMJ fibrocartilage engineering. *Acta Biomater* **7**, 1710, 2011.
- Anderson, D.E., and Athanasiou, K.A. A comparison of primary and passaged chondrocytes for use in engineering the temporomandibular joint. *Arch Oral Biol* **54**, 138, 2009.
- Anderson, D.E., and Athanasiou, K.A. Passaged goat costal chondrocytes provide a feasible cell source for temporomandibular joint tissue engineering. *Ann Biomed Eng* **36**, 1992, 2008.
- Mastrangelo, A.N., Magarian, E.M., Palmer, M.P., Vavken, P., and Murray, M.M. The effect of skeletal maturity on the regenerative function of intrinsic ACL cells. *J Orthop Res* **28**, 644, 2010.
- Murphy, M.K., Arzi, B., Hu, J.C., and Athanasiou, K.A. Tensile characterization of porcine temporomandibular joint disc attachments. *J Dent Res* **92**, 753, 2013.
- Carson, F.L. *Histotechnology: A Self-Instructional Text*, 2nd ed. Chicago, IL: ASCP Press, 1997.
- Bank, R.A., Beekman, B., Verzijl, N., de Roos, J.A., Sakke, A.N., and TeKoppele, J.M. Sensitive fluorimetric quantitation of pyridinium and pentosidine crosslinks in biological samples in a single high-performance liquid chromatographic run. *J Chromatogr B Biomed Sci Appl* **703**, 37, 1997.

23. Walpole, S.C., Prieto-Merino, D., Edwards, P., Cleland, J., Stevens, G., and Roberts, I. The weight of nations: an estimation of adult human biomass. *BMC Public Health* **12**, 439, 2012.
24. Kim, H., Song, K.D., Kim, H.J., Park, W., Kim, J., Lee, T., Shin, D.H., Kwak, W., Kwon, Y.J., Sung, S., Moon, S., Lee, K.T., Kim, N., Hong, J.K., Eo, K.Y., Seo, K.S., Kim, G., Park, S., Yun, C.H., Kim, H., Choi, K., Kim, J., Lee, W.K., Kim, D.K., Oh, J.D., Kim, E.S., Cho, S., Lee, H.K., Kim, T.H., and Kim, H. Exploring the genetic signature of body size in Yucatan miniature pig. *PLoS One* **10**, e0121732, 2015.
25. Detamore, M.S., and Athanasiou, K.A. Tensile properties of the porcine temporomandibular joint disc. *J Biomech Eng* **125**, 558, 2003.
26. Minarelli, A.M., Del Santo Junior, M., and Liberti, E.A. The structure of the human temporomandibular joint disc: a scanning electron microscopy study. *J Orofac Pain* **11**, 95, 1997.
27. Clement, C., Bravetti, P., Plenat, F., Foliguet, B., Haddioui, A.E., Gaudy, J.F., and Weissenbach, M. Quantitative analysis of the elastic fibres in the human temporomandibular articular disc and its attachments. *Int J Oral Maxillofac Surg* **35**, 1120, 2006.
28. Bermejo, A., Gonzalez, O., and Gonzalez, J.M. The pig as an animal model for experimentation on the temporomandibular articular complex. *Oral Surg Oral Med Oral Pathol* **75**, 18, 1993.
29. Henderson, S.E., Desai, R., Tashman, S., and Almarza, A.J. Functional analysis of the rabbit temporomandibular joint using dynamic biplane imaging. *J Biomech* **47**, 1360, 2014.
30. Sun, Z., Liu, Z.J., and Herring, S.W. Movement of temporomandibular joint tissues during mastication and passive manipulation in miniature pigs. *Arch Oral Biol* **47**, 293, 2002.
31. Ness, G.M. Arthroplasty and disectomy of the temporomandibular joint. *Atlas Oral Maxillofac Surg Clin North Am* **19**, 177, 2011.
32. Venn, M., and Maroudas, A. Chemical composition and swelling of normal and osteoarthrotic femoral head cartilage. I. Chemical composition. *Ann Rheum Dis* **36**, 121, 1977.
33. Makris, E.A., MacBarb, R.F., Paschos, N.K., Hu, J.C., and Athanasiou, K.A. Combined use of chondroitinase-ABC, TGF-beta1, and collagen crosslinking agent lysyl oxidase to engineer functional neotissues for fibrocartilage repair. *Biomaterials* **35**, 6787, 2014.
34. Kopp, S. Topographical distribution of sulphated glycosaminoglycans in human temporomandibular joint disks. A histochemical study of an autopsy material. *J Oral Pathol* **5**, 265, 1976.
35. Messineo, L., Denko, C.W., and Petricevic, M. Age-related changes in total DNA and RNA and incorporation of uridine and thymidine in rat liver, kidney and spleen. *Int J Biochem* **15**, 1103, 1983.
36. Ficklin, T., Thomas, G., Barthel, J.C., Asanbaeva, A., Thonar, E.J., Masuda, K., Chen, A.C., Sah, R.L., Davol, A., and Klisch, S.M. Articular cartilage mechanical and biochemical property relations before and after in vitro growth. *J Biomech* **40**, 3607, 2007.
37. Aladin, D.M., Cheung, K.M., Ngan, A.H., Chan, D., Leung, V.Y., Lim, C.T., Luk, K.D., and Lu, W.W. Nanostructure of collagen fibrils in human nucleus pulposus and its correlation with macroscale tissue mechanics. *J Orthop Res* **28**, 497, 2010.
38. Parry, D.A., Barnes, G.R., and Craig, A.S. A comparison of the size distribution of collagen fibrils in connective tissues as a function of age and a possible relation between fibril size distribution and mechanical properties. *Proc R Soc Lond B Biol Sci* **203**, 305, 1978.
39. Li, L.P., Buschmann, M.D., and Shirazi-Adl, A. Strain-rate dependent stiffness of articular cartilage in unconfined compression. *J Biomech Eng* **125**, 161, 2003.
40. Tanaka, E., and van Eijden, T. Biomechanical behavior of the temporomandibular joint disc. *Crit Rev Oral Biol Med* **14**, 138, 2003.
41. Shi, C., Wright, G.J., Ex-Lubeskie, C.L., Bradshaw, A.D., and Yao, H. Relationship between anisotropic diffusion properties and tissue morphology in porcine TMJ disc. *Osteoarthritis Cartilage* **21**, 625, 2013.
42. van der Laan, J.W., Brightwell, J., McAnulty, P., Ratky, J., Stark, C., and Steering Group of the, RETHINK Project. Regulatory acceptability of the minipig in the development of pharmaceuticals, chemicals and other products. *J Pharmacol Toxicol Methods* **62**, 184, 2010.
43. Colleton, C., Brewster, D., Chester, A., Clarke, D.O., Heining, P., Olaharski, A., and Graziano, M. The use of minipigs for preclinical safety assessment by the pharmaceutical industry: results of an IQ DruSafe minipig survey. *Toxicol Pathol* **44**, 458, 2016.

Address correspondence to:
 Kyriacos A. Athanasiou, PhD
 Department of Biomedical Engineering
 University of California, Davis
 Davis, CA 95616

E-mail: athanasiou@ucdavis.edu

Received: March 30, 2017

Accepted: May 23, 2017

Online Publication Date: July 6, 2017